Available online at www.sciencedirect.com

SciVerse ScienceDirect

Acta Materialia 61 (2013) 2121–2132

Acta MATERIALIA

www.elsevier.com/locate/actamat

Stability of binary nanocrystalline alloys against grain growth and phase separation

Heather A. Murdoch, Christopher A. Schuh *

Department of Materials Science and Engineering, MIT, Cambridge, MA 02139, USA

Received 27 August 2012; received in revised form 20 December 2012; accepted 23 December 2012
Available online 23 January 2013

Abstract

Grain boundary segregation has been established through both simulation and experiments as a successful approach to stabilize nanocrystalline materials against grain growth. However, relatively few alloy systems have been studied in this context; these vary in their efficacy, and in many cases the stabilization effect is compromised by second phase precipitation. Here we address the open-ended design problem of how to select alloy systems that may be stable in a nanocrystalline state. We continue the development of a general "regular nanocrystalline solution" model to identify the conditions under which binary nanocrystalline alloy systems with positive heats of mixing are stable with respect to both grain growth (segregation removes the grain boundary energy penalty) and phase separation (the free energy of the nanocrystalline system is lower than the common tangent defining the bulk miscibility gap). We calculate a "nanostructure stability map" in terms of alloy thermodynamic parameters. Three main regions are delineated in these maps: one where grain boundary segregation does not result in a stabilized nanocrystalline structure, one in which macroscopic phase separation would be preferential (despite the presence of a nanocrystalline state stable against grain growth) and one for which the nanocrystalline state is stable against both grain growth and phase separation. Additional details about the stabilized structures are also presented in the map, which can be regarded as a tool for the design of stable nanocrystalline alloys.

Keywords: Nanocrystalline alloys; Grain boundary segregation; Thermodynamic stability

1. Introduction

Pure nanocrystalline metals generally lack structural stability due to the excess energy associated with their high volume fraction of grain boundaries, often exhibiting grain growth, even at room temperature [1]. However, the addition of solute atoms can stabilize the nanostructure against grain growth. The mechanism for this improvement in stability has been proposed to involve the reduction of grain boundary energy through the segregation of solute atoms to the grain boundaries [2–5], with possible secondary kinetic contributions based on solute drag [6–10]. Accordingly, alloying has emerged as a critical component for the development and deployment of nanocrystalline materials, although our basic understanding of stability in nanocrystalline alloys remains incomplete.

Atomistic simulations on nanocrystalline alloys show that structural stabilization is contingent upon the distribution and character of the solute atom. A certain minimum concentration of solute is often found to be necessary for grain size stabilization, as for various solute species in simulated copper [11–17]. The efficacy of different solute species is variable, and in some studies has been related to the size difference between solute and solvent atoms [11–13]. However, in these studies, the grain boundaries are manually decorated with solute atoms, which may represent artificial segregation states. There have been fewer simulation works on systems where segregation is thermodynamic (by, e.g., Monte Carlo methods) [16–20]. These suggest that equilibrium solute segregation lowers the grain boundary energy to varying degrees. Examples include

* Corresponding author.
E-mail address: schuh@mit.edu (C.A. Schuh).

1359-6454/$36.00
http://dx.doi.org/10.1016/j.actamat.2012.12.033

simulations of bismuth and silver dopants in copper, where the energy associated with the grain boundaries varies across types of sites for grain boundary segregation, leading to segments of grain boundaries with lowered energy [16,17], a significant reduction in grain boundary energy (even to negative values) in Al–Pb systems [18,19] and simulations of tungsten segregation in nickel where a reduction in grain boundary energy of ~60% was observed [20].

Experimentally, a reduction in the propensity for grain growth in nanocrystalline materials has been observed in a variety of binary alloys [21–31]. There are many indications in experimental systems that there is a "preferred" grain size which emerges during processing which is closely linked to the solute content [2,24,30,32,33]; this is considered significant evidence for a thermodynamic contribution to stabilization. The grain size that is stable against coarsening is correlated to the solute concentration in these systems, but the system also often exhibits instabilities with respect to phase separation. In particular, the precipitation of a second phase above a certain solute content disturbs the segregation state and can trigger rapid grain growth [30,31,33,22,34].

The above studies using experiment and simulation have achieved varying levels of success on specific individual alloy systems. However, the total number of alloy systems studied is small, and there is not enough information to be able to extrapolate to other alloying elements in unexplored systems. Perhaps the best hope of providing a general understanding of this problem lies in the use of analytical thermodynamic modeling. A number of models pertaining to grain boundary segregation in nanocrystalline systems have been developed.

Starting from the Gibbs adsorption equation, Weissmüller noted that the segregation of solute atoms to the grain boundaries in a dilute system reduces the grain boundary energy, γ [3,4]:

$$\gamma = \gamma_0 - \Gamma(\Delta H^{seg} - kT\log[X]) \quad (1)$$

where the reduction in grain boundary energy from the unalloyed condition, γ_0, is a function of the heat of segregation for the binary system (ΔH^{seg}) and the solute excess (Γ) at the grain boundary for a particular global solute concentration (X) and temperature (T), with k the Boltzmann constant. Weissmüller considered the condition where $\gamma = 0$, which would eliminate the driving force for grain growth. He specifically included a consideration of the high fraction of grain boundary atoms in nanocrystalline materials, which leads to a large number of segregation sites, and calculated that there could be a nanocrystalline grain size fully stabilized ($\gamma = 0$) by solute segregation. The proposed composition of solute required for Weissmüller's "stable nanocrystalline" state varies across materials systems and models. Kirchheim performed a similar analytical derivation assuming an ideal dilute solution, and used it to formulate a relationship proposing an equilibrium grain size as a function of temperature [2,35], which has been applied to interpret data from a handful of experimental systems [2,33]. Meng and coworkers proposed a semi-empirical model for the distribution of solute in the segregating systems Fe–P, Fe–C and Al–Cu. Using experimental data from these systems as input, they predicted the distribution of solute, an increase in solute solubility with a decrease in grain size and that the precipitation temperature of an ordered compound can be suppressed for these systems [36]. Darling and coworkers adapted a model of surface segregation energy to evaluate potential alloying elements with iron on the basis of their propensity to lower grain boundary energy [26,28,37].

A more general, and generalizable, model is that of Trelewicz and Schuh [38], who proposed a regular nanocrystalline solution (RNS) model for the free energy of mixing in binary alloys with both crystalline and intercrystalline atomic environments. The RNS model reduces properly to a regular solution model for the crystalline phase in the limit of infinite grain size, and to a standard grain boundary segregation isotherm in the dilute limit. In principle it can provide an understanding of systems with any finite grain size at any solute level, given a few material-specific regular solution parameters, such as pairwise interactions, atomic volume and pure-component grain boundary energies. The RNS model is thus a generic thermodynamic approach that applies broadly to many alloy systems, and in fact could be used to help identify promising systems which can be stable in a nanocrystalline state.

The RNS model was explored parametrically in Ref. [38], and while the grain size–solute content relationships it predicted were promising with respect to experimental evidence, the stability of nanocrystalline systems was evaluated only with respect to changes in grain size. In fact, all of the analytical models described above suffer this deficiency as well. Clearly, suppression of grain growth is an important criterion for stabilizing a nanostructured alloy, but a potentially equally important stability is that with respect to phase separation. Even if a nanocrystalline alloy with grain boundary segregation is relatively more stable than a coarse-grained alloy of the same composition, the nanocrystalline state may never be achievable if the system phase separates. Additionally, as noted above, experimental studies suggest that second phase formation is often the principal instability seen in alloyed nanocrystalline systems, being an immediate precursor to runaway grain growth.

In a recent preliminary letter, we provided a first step towards understanding the stability of nanocrystalline systems against both coarsening and phase separation [39]. Specifically, we further developed the RNS model to explore phase separation in systems with positive heats of mixing. In that work, we limited our attention to a specific set of alloys based on tungsten, and did not explore the full configuration space available for all alloy systems. The purpose of the present work is to generalize our preliminary results from Ref. [39], developing in far greater detail a

series of "nanostructure design maps" that provide basic guidance on which alloys are most stable in a nanocrystalline solid solution configuration.

2. Theory

2.1. The regular nanocrystalline solution (RNS) model

To examine the phase separating behavior in bulk nanocrystalline systems stabilized via grain boundary segregation we use the free energy function based on the RNS model developed by Trelewicz and Schuh [38]. The model defines a grain boundary region (gb) and a "crystal" region in the grain interior (c) with the total solute concentration, X, satisfying the balance [40]:

$$X = f_{gb}X_{gb} + (1 - f_{gb})X_c \tag{2}$$

where X_{gb} is the concentration of solute species in the grain boundary region, X_c is the concentration in the grains and f_{gb} is the volume fraction of the grain boundary region:

$$f_{gb} = 1 - \left(\frac{d-t}{d}\right)^D \tag{3}$$

where d is the grain diameter, t is the thickness of the grain boundary region (taken to be 0.5 nm [38,41] throughout) and D is the dimensionality of the grain structure (taken to be $D = 3$ for this work). The model also defines a transition region composed of the bonds between the atoms in the grain and in the grain boundary region.

The analytical developments of Trelewicz and Schuh are statistical, and envision the system as a grid of atoms and bonds, as illustrated on the left of Fig. 1. In the end, the result is more general and the system can be viewed in a continuum fashion as on the right of Fig. 1. The spatial distribution of atomic bonds between the three regions, the energies associated with creating grain boundaries and region-weighted entropic contributions are encapsulated in the final free energy function derived from the model:

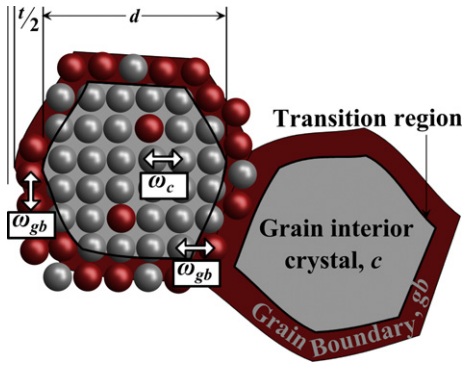

Fig. 1. Schematic of two nanocrystalline grains exhibiting grain boundary segregation, viewed equivalently as an array of atoms (left) or as a continuum (right). Gray atoms are solvent and red atoms are solute. The characteristic size of the grain, d, and grain boundary thickness, t, are shown, and the arrows denote the bonds associated with the interaction parameters used in the model.

$$\Delta G^{mix} = (1 - f_{gb})\Delta G_c^{mix} + f_{gb}\Delta G_{gb}^{mix} + zvf_{gb}(X_{gb} - X_c)\left[(2X_{gb} - 1)\omega_{gb} - \frac{1}{zt}(\Omega^B\gamma^B - \Omega^A\gamma^A)\right] \tag{4}$$

where z is the coordination number of the bulk material, Ω is the atomic volume, v is the transitional bond fraction (the fraction of atoms contributing bonds to the transitional bonding region) and ω is the interaction parameter defined:

$$\omega = E^{AB} - \frac{E^{AA} + E^{BB}}{2} \tag{5}$$

Two separate interaction parameters are used to describe the binary nanocrystalline system: a bulk parameter ω_c describing the crystal and ω_{gb} describing the interactions in the grain boundary and transition regions. This grain boundary interaction may or may not differ in character from that in the bulk, and its significance will be discussed further in later sections. A positive interaction parameter denotes a phase separating system, where the energy of AB bonds is greater than the average of AA and BB bonds. It relates to the heat of mixing of a regular solution via:

$$\Delta H^{mix} = z\omega_c X(1 - X) \tag{6}$$

The miscibility gap of a system with a larger interaction parameter exhibits a higher critical temperature and a lower solubility limit.

The terms ΔG_c^{mix} and ΔG_{gb}^{mix} represent the outer bounds of the system. If the material is composed only of crystal, i.e., grain interior ($d \to \infty$, $f_{gb} \to 0$), the free energy function reduces to simply that of a classical regular solution:

$$\Delta G_c^{mix} = z\omega_c X_c(1 - X_c) + kT[X_c \ln X_c + (1 - X_c)\ln(1 - X_c)] \tag{7}$$

In the lower limit of grain size ($d = t$) is the free energy term of the grain boundary regular solution, which also includes a dependence on the pure grain boundary energies of both species:

$$\Delta G_{gb}^{mix} = z\omega_{gb}X_{gb}(1 - X_{gb}) + \frac{\Omega^A\gamma^A}{t}(1 - X_{gb}) + \frac{\Omega^B\gamma^B}{t}X_{gb} + kT[X_{gb}\ln X_{gb} + (1 - X_{gb})\ln(1 - X_{gb})] \tag{8}$$

The remaining terms in Eq. (4) describe the transition region. In Ref. [38], Trelewicz showed the value of the RNS model in identifying nanocrystalline alloys with segregation states that lead to formal stability against coarsening. The signature output of the model is a free-energy surface of the kind shown in Fig. 2, plotted as a function of grain size (d) and grain boundary concentration (X_{gb}) at a constant global solute content and temperature. For certain combinations of input parameters (interaction parameters ω, global concentration and temperature), the

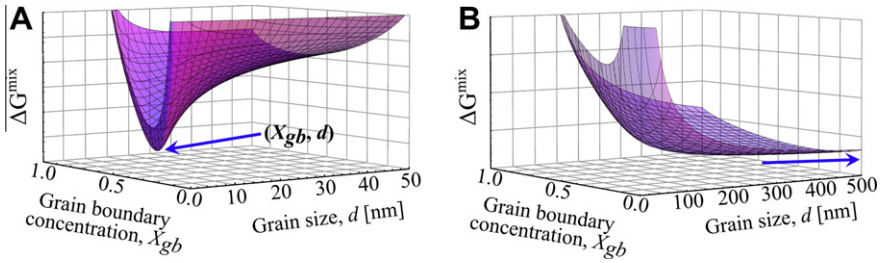

Fig. 2. (A) Gibbs free energy of mixing surface for a single value of global solute concentration. The minimum of the curve (shown magnified in Fig. 3) represents a grain size and grain boundary solute concentration at which the grain boundary energy for the given global solute concentration is zero. (B) A free energy surface calculated from different thermodynamic inputs, with no nanocrystalline minimum present. The minimum value corresponds to that of the bulk regular solution (infinite grain size).

free-energy surface can exhibit a global minimum at a pair value of (X_{gb}, d), for which the nanocrystalline microstructure is stable (Fig. 2A). The minimum on the concentration axis (X_{gb}) shows the segregation state that is neither over- nor under-full (i.e., ideally saturated with solute). The minimum with respect to grain size corresponds to an alloy grain boundary energy of zero, and describes a nanostructure that is stable with respect to grain growth.

The existence of a minimum in the free energy surface depends on the material's parameters and the solute content of the system. There are many cases where a nontrivial minimum does not exist (Fig. 2B), for which the "preferred" grain size is infinite, and the free energy of the system matches that of a bulk regular solution for the same global solute content.

3. Methods

Our interest in this paper is to adapt the RNS model outlined above to consider the stability of nanocrystalline systems not only against grain growth, but also against phase separation. A key concept required to do this is the comparison of a given minimum-energy configuration of the kind shown in Fig. 2A, which only considers segregated nanocrystalline solid solution configurations for a single composition, against other possible configurations that include phase separation.

In order to appreciate how such comparisons are made, consider the free energy surface constructed for a discrete value of global solute content, i.e., of the kind shown in Fig. 2A, with a minimum at a given value of grain boundary composition and grain size, (X_{gb}, d). In Fig. 3, we examine the region of the minimum in such a surface with greater detail. Consider what happens if we hold these values of X_{gb} and d constant, and vary the global composition, X. For the purposes of illustration, consider two global compositions, X^+ and X^-, slightly different from one another, which we can compare. At the global concentration X^+, a minimum occurs in the free energy surface (lower curve in Fig. 3) at a specific value of grain boundary concentration and grain size, (X^+_{gb}, d^+). If we decrease the global composition to X^- for the values (X^+_{gb}, d^+), the free energy increases; it turns out that this increase is extremely

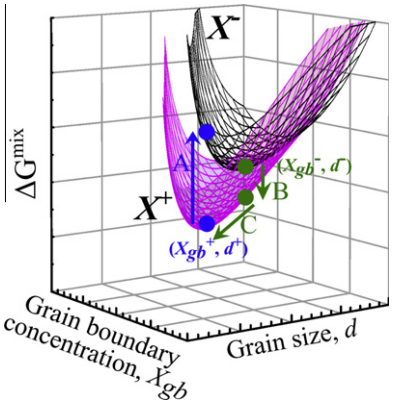

Fig. 3. Minima in the free energy surface for two global solute concentrations, X^+ and X^-. Starting at the minimum for the X^+ curve (magenta), if the grain size and grain boundary concentration, X_{gb}, are held constant, and the global solute content is decreased to X^-, the free energy increases rapidly (arrow A). Starting at the minimum of the X^- curve (black), if the grain size and X_{gb} are held constant for an increase in global solute content (arrow B), the free energy decreases; however, the grain boundary energy at this point is negative, indicating a desire to increase grain boundary area (arrow C). See Fig. 4 for an alternate presentation.

rapid with respect to even small changes in global composition (Fig. 3, arrow A). We note that this is similar to the free energy behavior of a stoichiometric line compound phase, with a single preferred composition for which the energy is minimized. If we instead start with the global composition X^-, with the minimum at (X^-_{gb}, d^-) and increase the composition (Fig. 3, arrow B), the grain boundary energy drops to less than zero, indicating that the grain size would prefer to decrease. On this new free energy surface for the higher composition (X^+), the system can decrease its energy by obtaining a new minimum (Fig. 3, arrow C) at a smaller grain size.

We may also examine these trends on other axes; if we plot the variation in free energy with respect to global composition, X, for a fixed pair of X_{gb} and d (Fig. 4), we can also see the sharp increase in free energy upon moving to the left, and the free energy decrease obtained by decreasing grain size to a new free-energy curve (with different values of X_{gb} and d). It is important to note that the shapes of the free energy curves in Fig. 4 are such that they are

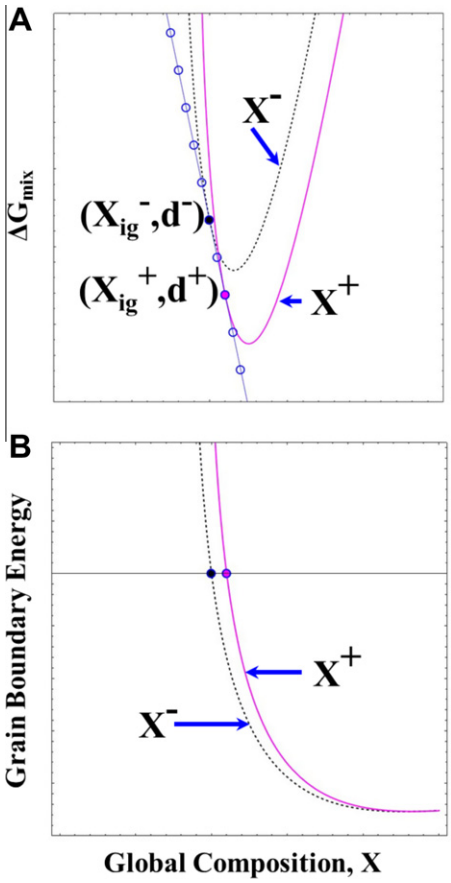

Fig. 4. (A) Blue points represent the minimum in the free energy surface at each value of global composition. For the values of X^- (dashed) and X^+ (solid), the values of grain size and the grain boundary solute content that comprise the minimum for that global composition are held constant while the global composition is varied. The blue line shows that the minima points are the tangents between set X_{gb}/d value curves. (B) Grain boundary energy as a function of global composition for the X_{gb} and d values for same two minima as denoted in (A) and Fig. 3. (For interpretation of the references to color in this figure legend, the reader is referred to the web version of this article.)

connected by a common tangent (blue line, Fig. 4) between curves at set values of X_{gb} and d. This means that the system prefers to exist at the combination of grain size and grain boundary solute content that is the minimum of a free energy surface for a given global composition (blue circle).

Based on the above discussion, we can think about nanocrystalline alloys in an equilibrium grain boundary segregation state in the following way: we may treat the minimum of the free energy surface at each global composition as a "stoichiometric line compound", represented by a point. In other words, for each composition X, there is one preferred "compound" with a given grain boundary concentration and grain size, (X_{gb}^-, d^-). If the global composition is changed, there is a different preferred combination (X_{gb}^+, d^+), and the system resembles a different "compound". When free energy curves are plotted against X, as is traditional in the development of binary phase diagrams, then these points may be compared to the free energy functions of other competing phases. This is taken up in detail in the next section.

3.1. RNS for phase separating systems

Fig. 5 shows the general problem that is the focus of this paper: comparing the minimum-energy nanocrystalline system free energy curve, as developed above, with those of competing phases. We are specifically concerned with the case where the competing phases are the classical bulk (i.e., non-nanocrystalline) phases, and for simplicity we concern ourselves only with positive heat of mixing systems. Additionally, we represent the bulk solid solution with one classical, symmetric regular solution phase that describes both the solvent- and solute-rich solutions; a schematic free energy curve for such a bulk system at a single finite temperature is shown by the solid black line in Fig. 5, with the two-phase field corresponding to the region between the tangent points of the common tangent line (dashed black line).

This curve, and the two phases represented by it, may be compared with the very narrow U-shaped curve associated with a specific nanocrystalline state, as shown schematically by the blue curves. More specifically, as described above, we view the nanocrystalline state as a "compound" at a specific point, denoted explicitly by a blue solid point in Fig. 5. Depending upon the specific input parameters used, the location of this point can fall into one of three main regions that are delineated in Fig. 5: "stable nanocrystalline", "metastable nanocrystalline" and "nanocrystalline not supported". Those with minima at a free energy lower than the common tangent of the bulk regular solution limit are labeled as "stable nanocrystalline"; those where the minimum of the free energy surface is the trivial case of infinite grain size and the same free energy of the bulk (non-nanostructured) solid solution occupy the "nanocrystalline not supported" region. Nanocrystalline states that have a free energy lower than the bulk free

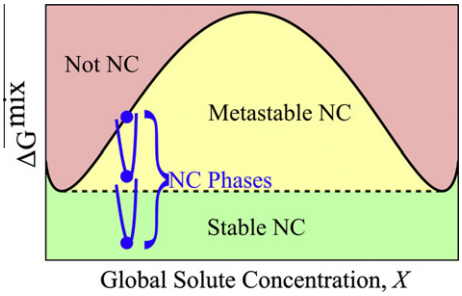

Fig. 5. The free energy of the nanocrystalline (NC) phases can fall into three regions that are determined by the bulk regular solution (black curve) for the same materials parameters. If there is no minimum in the free energy surface, it is "Not NC". If the free energy surface has a minimum, but its free energy falls above the common tangent of the bulk system (denoting phase separation, dashed black line), it is "Metasable NC". A stable nanocrystalline system falls below the common tangent.

energy curve, but higher than its common tangent, are labeled as "metastable nanocrystalline". In this latter case, the nanocrystalline structure is more energetically favorable than the single phase solid solution at that solute content, but less favorable than macroscopic phase separation of the system into two solid solutions.

3.2. Parameterization

As we are currently exploring only phase separating systems described by symmetric regular solid solutions, we use positive values for the crystal pair-wise interaction parameter, ω_c, that correspond to enthalpies of mixing (Eq. (6)) from 1 to 150 kJ mol^{-1}. For simplicity, we take the combination of grain boundary energy and atomic volume, divided by the grain boundary thickness, $\Omega\gamma/t$ (which are always together in the RNS model) of the two pure species to be equal; in the free energy equation, the terms containing these parameters are generally on the order of a tenth the magnitude of the other terms, and less when they appear together as a difference. We select a value for the term $\Omega\gamma/t$ of 8.25 kJ mol^{-1} for both solvent and solute; this corresponds, for example, to a grain boundary energy of 0.5 J m^{-2}, an atomic volume of 8.25 cm^3 mol^{-1} and a grain boundary thickness of 0.5 nm. (For reference, the values of $\Omega\gamma/t$ for some common metals are aluminum: 6.5, gold: 7.7, copper: 8.9, iron: 10.6, and nickel: 11.5 kJ mol^{-1}.)

The last variable needed to implement the model is ω_{gb}, which describes the character of atomic interactions in the grain boundary and transition regions (Fig. 1). In general the grain boundary interaction parameter will be different from the grain interaction parameter; this in fact is the driving force for grain boundary segregation, as the enthalpy of segregation is:

$$\begin{aligned}\Delta H^{seg} = z\left[\omega_c - \omega_{gb}\left(1-\frac{v}{1-f_{gb}}\right) - \frac{1}{zt}\left(\Omega^B\gamma^B - \Omega^A\gamma^A\right)\left(1-\frac{v}{1-f_{gb}}\right)\right] \\ + 2zX_{gb}\omega_{gb}\left(1-\frac{v}{1-f_{gb}}\right) \\ - 2z\left[X_c\omega_c + v\left(X_{gb}-X_c\right)\omega_{gb}\right]\end{aligned} \tag{9}$$

which comes from the segregation isotherm that emerges from the RNS model [38]:

$$\frac{X_{gb}}{1-X_{gb}} = \frac{X_c}{1-X_c}\exp\left[\frac{\Delta H^{seg}}{kT}\right] \tag{10}$$

Note that the convention is a positive value for the enthalpy of segregation for a system in which the solute preferentially segregates to the grain boundaries. If the segregation enthalpy in Eq. (9) is taken to the dilute limit:

$$\Delta H_0^{seg} = z\left(\omega_c - \frac{\omega_{gb}}{2} - \frac{\Omega^B\gamma^B - \Omega^A\gamma^A}{2zt}\right) \tag{11a}$$

we have a relationship between all of the parameters in this study and a dilute heat of segregation which is a measurable (or estimable) quantity. In the present work our assumption of $\Omega^A\gamma^A = \Omega^B\gamma^B$ reduces this equation further:

$$\Delta H_0^{seg} = z\left(\omega_c - \frac{\omega_{gb}}{2}\right) \tag{11b}$$

The grain boundary interaction parameter was varied to give ΔH_0^{seg} values between 1 and 150 kJ mol^{-1}. Given the other values for the parameters appearing in Eq. (11), this means that ω_{gb} can take on values both positive and negative. Depending on the magnitude of ω_c, a strongly segregating system would have either a positive grain boundary interaction parameter of significantly less magnitude than ω_c or a negative grain boundary interaction parameter.

Lastly, we must define a temperature at which we compare the nanocrystalline and other phases. In this paper, we primarily discuss results generated for the temperature $0.35T_{cr}$, where T_{cr} is the critical temperature defined at the top of the miscibility gap, and a direct relation to ω_c ($T_{cr} = z\omega_c/2R$); extension to other temperatures is straightforward – two more fractional temperatures, 0.5 and 0.65, are considered in this work as well.

By varying the two interaction parameters with high resolution (down to intervals of 0.001 eV) across the ranges described above, we have numerically calculated the minimum free energy curves for 100 compositions evenly spaced across the full range ($X = 0$–1). These minima are plotted against the bulk regular solution free energy curve with the same values of ω_c and z (exactly as in Fig. 5). We next examine the characteristics of material systems that have stable, metastable or no stable nanocrystalline states. The next few sections discuss these situations in terms of their general features, but do not focus on specific numerical values of the input parameters. Later in the paper, all of these results are synthesized into a quantitative nanostructure stability map that summarizes when these various situations arise.

4. Bulk phase stability

There are two general cases in which a system has no stable nanocrystalline configuration. The first and most trivial case to consider is the one where there is no free energy curve with a minimum at a finite grain size for any of the possible compositions. This is the situation pictured in Fig. 2B, and arises in cases where the heat of segregation is insufficiently large with respect to the value of the heat of mixing. Therefore, no energy minimum exists over the entire range of composition because the alloying interactions in the grain boundary are not sufficiently different from those in the grains to drive solute segregation.

With regards to the second case, systems which have nanocrystalline energy minima across a wide range of composition (and energies either stable or metastable with

respect to phase separation) still have composition ranges where the nanocrystalline state is not stable. Specifically, when the global composition is below the solubility limit, we do not identify any stable nanocrystalline compounds, for any of the materials parameter permutations in this study. In other words, in phase separating alloys, supersaturated solid solutions are required to achieve a fully nanocrystalline structure stable against grain growth. In this connection, it is interesting to note that some of the prior analytical models of segregation in nanocrystalline systems, such as those by Weissmüller [3,4] and Kirchheim [2] require the assumption of a dilute limit. Our calculations reveal that this is problematic for alloys with positive heats of mixing, and non-dilute solubility limits. We next examine the cases in which nanocrystalline minima exist in the free energy surface.

5. Stability

We find that the types of nanostructures that are thermodynamically stable are diverse, and predominantly not the expected simple grain boundary-segregated single phase states (involving a decreasing grain size with increasing composition) of the kind widely discussed in the literature. We briefly discuss the several stable nanostructured states that can be uniquely identified on the basis of the present model.

5.1. Classical segregation-stabilized nanocrystalline region

For some combinations of high heats of mixing and high heats of segregation, we are able to achieve the condition of segregation-based nanostructure stabilization envisioned by Weissmüller [3,4]. In these cases the relationship between the enthalpies is such that the grain boundary interaction parameter approaches ideal behavior, namely $\omega_{gb} = 0$.

A representative free energy curve comparison can be seen in Fig. 6A. Here each blue point is a nanocrystalline "compound". In the magnified views of Fig. 6B and C we illustrate the local free-energy curves corresponding to a few such points, and note that the points corresponding to the stable condition all lie on a single common tangent line. The points shown are simply example concentrations, and there are in fact an infinite number of them between any two of those shown; the locus of the points represents a smooth continuum of stable grain sizes that are a monotonic function of the composition. In fact, the grain size decreases with increasing solute content in the relationship often observed in experimental systems (Fig. 6D).

What is interesting to note for systems of this type is that there is a well-defined composition range over which a nanocrystalline state is supported, with strict limits on either end. At low solute concentrations, the existence of

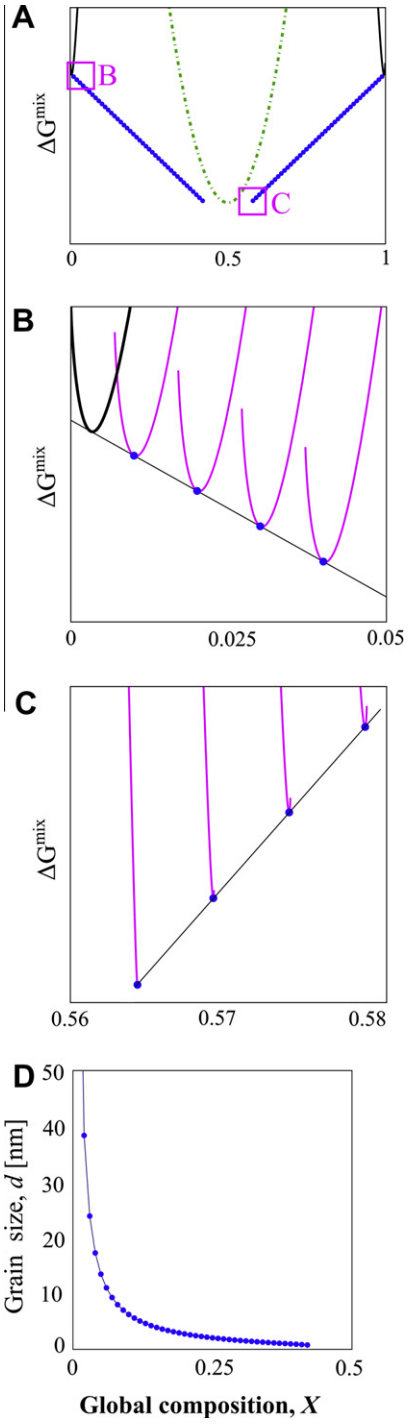

Fig. 6. (A) Free energy comparison of regular solution (curve), amorphous limit (dashed curve), and the nanocrystalline points (circles) for the "classical nanocrystalline" case. This example case has an enthalpy of mixing of 81 kJ mol^{-1} and enthalpy of segregation of 79 kJ mol^{-1}. (B) An enlarged view of the free energy comparison of nanocrystalline points as they approach the regular solution at the solubility limit, in the region marked in (A). (C) As in (B), enlarged scale free energy comparison of the terminus of the nanocrystalline points as indicated by the box in (A). The final composition that supports a nanocrystalline phase due to the (X_{gb}, d) space limitation is seen with respect to global composition. (D) Grain size versus global composition for the stable nanocrystalline alloys.

nanocrystalline states is bounded by the solubility limit, below which no nanocrystalline minima exist. This was already briefly discussed in Section 4, and can be seen graphically in the magnified view of Fig. 6B. For high concentrations of solute, the limiting composition is less physically obvious on the free energy diagram, but is inherent in the composition relationship in Eq. (2). For a given global composition, there is a limit to the (X_{gb}, d) combinations that can be supported while conforming to Eq. (2); if all of the solute is present in the grain boundaries and none in the grain interiors, $X = f_{gb}X_{gb}$ restricts the smallest grain size and largest value of solute allowable for a stable nanocrystalline phase. This limitation creates boundaries on the free energy surface, beyond which no surface exists; this can be seen in, e.g., Fig. 2A (on the left-hand side where the smallest grain sizes cannot be accessed on the free energy surface). This truncation of the free energy curves can also be seen in the magnified view in Fig. 6C, which shows the points for the nanocrystalline states close to the limiting composition, as well as their individual free energy curves; note that these are all truncated on the left-hand side, at the limits achievable by Eq. (2). The truncation becomes more and more severe as the concentration rises, and the last nanocrystalline compound – that with the largest possible solute content – is the last that has a minimum in the free energy surface contained within the available range of grain size and solute distribution (Fig. 6C). We will call this compound the "terminal" nanocrystalline structure.

The series of blue points that all lie on a common "nanocrystal free energy line" are a common feature of many systems, and in fact the arrangement of these lines in the free energy diagram leads to many possible unique situations. These lines, and particularly their terminal compositions, will play a major role in the discussion over the next few sections. In the case pictured in Fig. 6A, for example, these lines end at the terminal nanocrystalline structure, leaving a gap between their ends. These terminal structures have the lowest free energy in the system, far lower than that of the bulk regular solution. The nanocrystalline phases in this system are also in equilibrium with the bulk regular solution phase. For non-dilute alloys, there is a miscibility gap that separates the terminal solvent-rich nanocrystalline compound and its counterpart terminal solute-rich nanocrystalline compound. These nanocrystalline compounds are symmetric, due to our assumption of equal $\Omega\gamma/t$ for solvent and solute.

For the example system presented in this figure (and in other cases to be detailed in the following section), another apparent "phase" appears, shown by the green[1] dashed line in Fig. 6A. This free energy curve corresponds to the grain boundary regular solution (Eq. (8)) – the limit of the RNS model as grain size, d, approaches the grain boundary width, t, i.e., as the system approaches the "amorphous limit" where the material is entirely composed of grain boundary state. The situation can arise where the amorphous limit can be lower in energy in the central composition region where nanocrystalline states are not supported due to the (X_{gb}, d)-space limitations.

For these cases in the classical region, this leads to equilibrium between the terminal nanocrystalline compound and the amorphous limit phase (similarly, between the amorphous limit phase and the right-hand terminal nanocrystalline compound). The case where the amorphous limit exhibits a lower free energy than the nanocrystalline points such that it forms the lowest common tangent with the bulk regular solution is discussed in the following section.

5.2. Amorphous limit

In a range of cases, the "grain boundary phase" described above has the lowest free energy curve, as shown for an example case in Fig. 7, where this curve falls below the free energy lines of the nanocrystalline structures. This situation arises only when the grain boundary interaction parameter is strongly negative and the grain interaction parameter strongly positive; this drives the preference for grain boundary regions over crystalline ones. That the grain boundary term of the RNS could in fact have the lowest free energy of any other possible state suggests that there are positive heat of mixing systems in which an "amorphous" state is stable (due to its relatively lower heat of mixing). Interestingly, the idea of a stable amorphous phase is not new to this work [42], although the present RNS framework may provide a new way of looking at the development of amorphous alloys on the basis of their grain boundary segregation behavior. For example, in Fig. 7 we see that when the grain boundary phase is the lowest free energy state, it is in equilibrium with the bulk regular solution. This may relate to a common metric for assessing binary amorphous systems: the glass forming range (GFR). There are a number of approaches to estimate the GFR (i.e., size/structure difference, eutectic shape

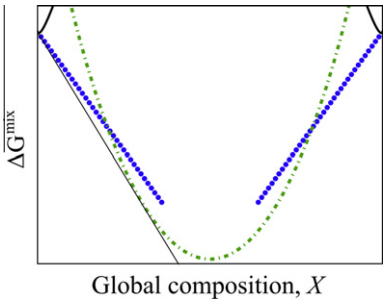

Fig. 7. The free energy of the amorphous phase (dashed curve) is lower than that of the bulk regular solution (solid curve) and the nanocrystalline points (circles). This example case has an enthalpy of mixing of 93 kJ mol^{-1} and enthalpy of segregation of 104 kJ mol^{-1}.

[1] For interpretation of color in Figs. 5, 6 and 11, the reader is referred to the web version of this article.

and enthalpy models) [42], and the present RNS model offers another approach.

5.3. Dual-phase nanocrystalline

In cases where the heat of segregation is larger than the heat of mixing, such that ω_{gb} is negative, but not sufficient to drive the system to the amorphous limit, the free energy surface at a given composition (Fig. 8B) supports two minima where the grain boundary energy is zero; hence the designation "dual-phase nanocrystalline". One of these minima is the classic grain boundary segregation-stabilized state – the solute is strongly segregated to the grain boundaries, and the stabilized grain size continues to decrease with an increase in composition along the nanocrystal free energy line; the second minimum has solute-rich grains with the solvent segregated to the grain boundary. Because ω_{gb} also describes the cross-interactions between the crystalline and grain boundary regions (recall Fig. 1), a mildly negative value of this parameter leads the system to maximize unlike bonds crossing between these regions. This in turn promotes a finer grain size, and in order to support the increased grain boundary volume, the grain boundary region must be occupied by the majority element (solvent).

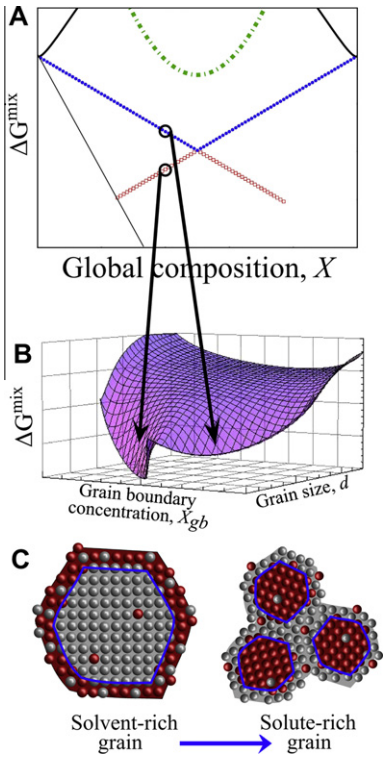

Fig. 8. (A) Free energy plot showing regular solution (solid curve), nanocrystalline phases with solute-rich grain boundaries (circles) and nanocrystalline phases where the solvent has become the grain boundary element (squares). This example case has an enthalpy of mixing of 23 kJ mol^{-1} and enthalpy of segregation of 35 kJ mol^{-1}. (B) Free energy surface for a given global solute composition showing the two minima. (C) Schematic of the nanostructure rearrangement from solvent-rich grains to solute-rich grains.

Thus, the roles of solute and solvent are exchanged and the preferred system is a "solute nanocrystalline phase". The composition range of such solute nanocrystalline phases is limited by the same (X_{gb}, d)-space constraints as the classical "solvent" nanocrystalline phases, discussed in Section 5.1. The solute nanocrystalline phases also follow a composition–grain size relationship; however, as the solute concentration decreases from the equiatomic concentration, the grain size decreases.

While we describe this case as "dual-phase nanocrystalline" due to the existence of two nanocrystalline phases stable against grain growth at a single composition, the solute nanocrystalline phase is lower in free energy. Constructing common tangents on Fig. 8 leads to the conclusion that over a broad range of compositions the solute nanocrystalline phase is in equilibrium with the bulk regular solution; on the solvent-rich side of the phase diagram, the stable states are a solvent-rich solid solution and a solute-rich nanocrystalline phase with grain boundary segregation. In the middle of the diagram, the equilibrium is between two solute nanocrystalline phases, which should be an interesting dual-phase nanocomposite that would in general be a true stable bimodal structure.

5.4. Dual-phase nanocrystalline/amorphous structures

In the previous two sections we have seen cases where the nanocrystalline points compete with an amorphous phase, or with one another (solute nanocrystalline phase). These cases correspond to a relatively higher and lower heat of mixing, respectively. Between these two extremes lies a condition in which both the grain boundary free energy curve (amorphous limit) and the terminal compositions of the nanocrystalline free energy lines are stable. An example of this situation is shown in Fig. 9, where the low energy of the grain boundary regions places it in equilibrium with the bulk regular solution at low solute levels. At higher concentrations, the amorphous limit is in equilibrium with the solute nanocrystalline phase defined by the terminal structures of the nanocrystal free energy lines.

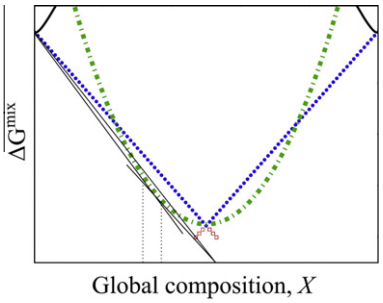

Fig. 9. Free energy plot for a case where the amorphous limit (dashed curve) appears below the common tangent (thin line) between the regular solution (thick solid curve) and nanocrystalline phases (solvent nanocrystalline phases in filled circles; solute nanocrystalline phases in open squares). This example case has an enthalpy of mixing of 58 kJ mol^{-1} and enthalpy of segregation of 75 kJ mol^{-1}.

The two solute nanocrystalline phases are in equilibrium around the equiatomic composition.

6. Metastable nanocrystalline alloys

In the case of metastable nanocrystalline structures, the RNS model reveals a minimum energy in the X_{gb}–d space, and grain size decreases with composition in a relationship similar to other model predictions and experimental data. However, these states are unstable with respect to macroscopic phase separation into the bulk phases. Fig. 10A typifies the free energy diagram of such a system, which comprises nanocrystalline free energy lines that lie below the regular solution free energy curve, but above the common tangent denoting bulk phase separation (the yellow region of Fig. 5). A nanocrystalline system in this condition would be stable against grain growth but would lower its energy via phase separation on the bulk scale.

However, the situation surrounding the free energy minima in this case is not quite the same as seen in our earlier analysis using X^+ and X^- for the case of a stable nanocrystalline structure. In that case, decreasing the composition at the set values of X_{gb} and d resulted in a sharp increase, and increasing the composition led to a lowering of the free energy through decreasing grain size. In the metastable case, the same types of behavior are seen, but with opposite composition tendencies (Fig. 10C and D). For an increase in composition, the free energy increases rapidly; for a decrease in composition, the grain boundary energy is positive, and as a result the system favors grain growth. This pattern continues until the infinite grain size of the regular solution is obtained (Fig. 10B). At the nanocrystalline compound values of X_{gb} and d the grain boundary energy has been reduced to zero, eliminating the drive for grain growth, but the free energy of a system with a larger grain size is always a lower free energy state. At the same time, the lower free energy of the common-tangent bulk phases dictates that the structure phase separate, so the equilibrium structure is a coarse-grained, phase-separated system.

7. Nanocrystalline stability map

The above discussion briefly delineated the types of behavior that emerge from the RNS model for positive heats of mixing. Which of these situations is relevant for a given alloy system depends principally upon its mixing parameters (in the grains and grain boundary region). Through the thousands of individual calculations conducted here, we are able to delineate regimes in the mixing-parameter space corresponding to each behavior

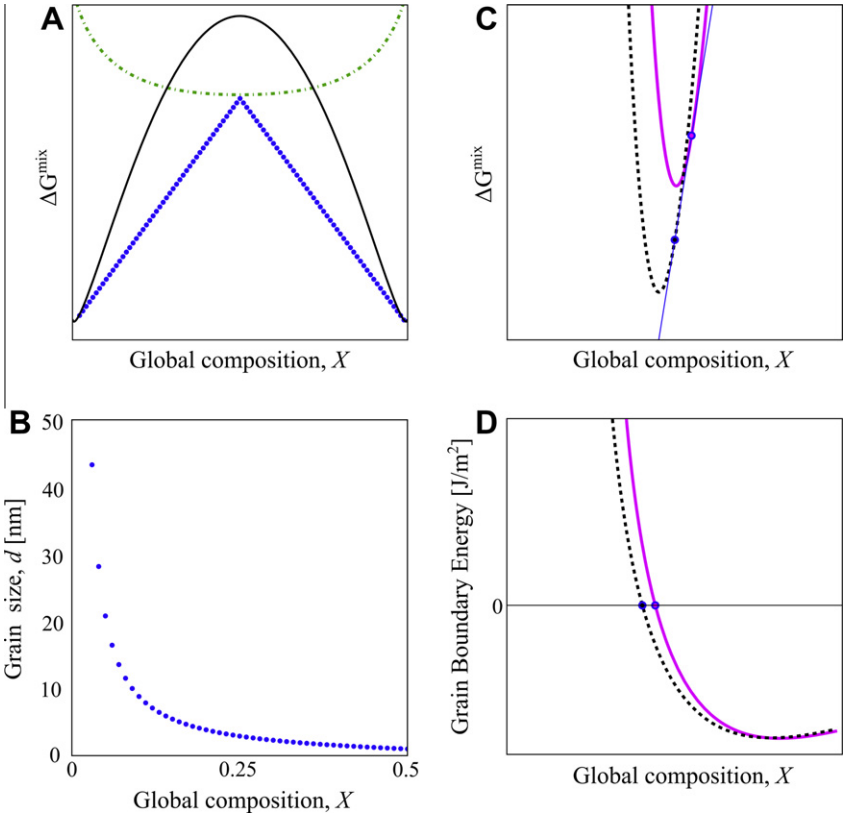

Fig. 10. (A) Free energy comparison of a regular solution (solid curve) and nanocrystalline points (circles). This example case has an enthalpy of mixing of 58 kJ mol^{-1} and enthalpy of segregation of 49 kJ mol^{-1}. (B) Grain size as a function of the global solute concentration in this metastable nanocrystalline binary alloy. (C) Similar to Fig. 4, the minima for two compositions are plotted as points, while the curves represent the free energy as a function of composition if the X_{gb} and d values for those minimum are held constant. (D) Grain boundary energy as a function of global composition for the X_{gb} and d values for the same two minima as denoted in (A).

described above. Although the heats of mixing (Eq. (6)) and grain boundary segregation (Eq. (11)) share terms associated with the bulk interaction parameter, the grain boundary interaction parameter is considered an independent quantity here, and only contributes to the heat of grain boundary segregation; the two parameters thus can be cast as the axes of the design space, as shown in Fig. 11. While in general the mixing parameters ω_c and ω_{gb} are more fundamental to the RNS model, these axes are more physically familiar, and therefore likely more useful in placing specific binary alloy systems on the map.

Interestingly, we find that the regions separating stability, metastability or unsuitability of a nanostructured alloy system are demarcated by straight lines in the double-logarithmic space of Fig. 11. While these lines are not of slope unity, they correspond to a power law, and can be empirically captured by the following relationship:

$$\frac{\Delta H^{seg}}{(\Delta H^{mix})^a} = c \tag{12}$$

where a is the power-law slope and c reflects the intercepts. Both of these are in general a function of temperature; for the map presented in Fig. 11, $T = 0.35T_{cr}$. For other temperatures investigated thus far (see Table 1), the map has the same basic form, but with shifted boundaries reflected in the different fitted values of a and c.

At the highest level, the map in Fig. 11 shows the tradeoff between grain boundary and bulk segregation tendencies as controlling the ability to stabilize a nanocrystalline phase. In fact, the power-law-modified ratio of the two quantities collected on the left-hand side of Eq. (12),

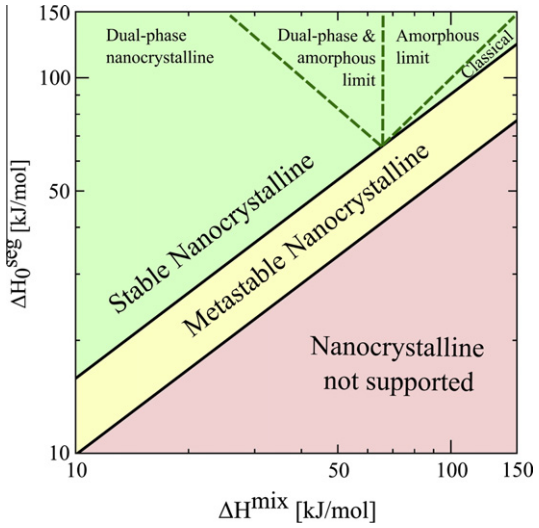

Fig. 11. Nanostructure stability map, presenting delineated regions of stability (green), metastability (yellow) and no stability (red) in binary alloys as a function of their enthalpies of mixing and segregation. The regions of behavior within the stable nanocrystalline region are defined in the text: dual-phase nanocrystalline (Section 5.3); amorphous and dual-phase (Section 5.4); amorphous limit (Section 5.2); classical stability (Section 5.1). Metastability is discussed in Section 6 and no stability is discussed in Section 4. This map is calculated for a fixed dimensionless temperature of $0.35T_{cr}$. (For interpretation of the references to color in this figure legend, the reader is referred to the web version of this article.)

Table 1
Fitted coefficients for the nanostructuring figure of merit, Eq. (12) at three dimensionless temperatures.

Temperature	a (slope)	c (intercepts)	
		Metastable	Stable
$0.35T_{cr}$	0.757	1.7326	2.768
$0.5T_{cr}$	0.661	2.8038	3.7236
$0.65T_{cr}$	0.567	4.425	4.958

$\Delta H^{seg}/(\Delta H^{mix})^a$ represents a useful figure of merit for binary systems' nanostructuring ability, with higher values lying more towards the upper-left of the stability map.

At a more nuanced level, the map is populated with subregions that correspond to the various unique cases delineated earlier. Specifically, the stable nanocrystalline region (green) is divided into four subspaces denoting the regions where the classical nanocrystalline, dual-phase nanocrystalline , amorphous limit and dual-phase nanocrystalline and amorphous limit, are the dominant cases. The classical grain-boundary segregation-based stabilized nanocrystalline state of the kind envisioned by Weissmüller [3,4] and Trelewicz and Schuh [38] and widely sought experimentally, represents a small sliver of the design space. This illustrates the challenge the field can expect to face in designing nanocrystalline alloys, at least in phase-separating binary systems. In our previous work [39], we briefly illustrate an example method to calculate the enthalpies necessary for populating the nanocrystalline design map with potential alloy systems; further work should aim to expand the number and types of alloys represented.

8. Conclusions

In this work, we have examined the requirements for a binary phase separating system to support a nanocrystalline structure stable against both grain growth and phase separation. The most salient results of this work include the following:

- In general, stable nanostructures occur at values of ΔH^{seg} that are high relative to ΔH^{mix}. More specifically, a figure of merit, $\Delta H^{seg}/(\Delta H^{mix})^a$, with a an exponent in the range ~0.5–1, delineates the regions of nanocrystalline stability, nanocrystalline metastability and bulk stability via temperature-dependent constants calculated in the present work for several fractional temperatures.
- Several types of nanostructures are stable, including not only the previously predicted segregation-stabilized nanocrystalline system, but also dual-phase nanostructures and an amorphous-type structure. These stable states exist at compositions greater than the bulk solubility limit.
- There is a range of alloys which supports a metastable nanocrystalline state – one in which the nanocrystalline structure is stable against grain growth (having a grain boundary energy of zero), but not against macroscopic phase separation.

- A considerable range of alloys are incapable of supporting a nanocrystalline state that is stable against grain growth.

All of these features are represented on nanostructure stability maps, which are constructed in this work for a particular set of temperatures and materials parameters. Using this method, maps can be generated for desired conditions to determine stable nanocrystalline alloys for a wide variety of applications. In addition to being practically relevant, the maps reveal new types of stable nanostructures for further investigation.

Acknowledgments

This research was supported primarily by the US Army Research Office under Contract W911NF-09-1-0422, with partial additional support from the Solid State Solar Thermal Energy Conversion (S3TEC), an Energy Frontier Research Center funded by the US Department of Energy, Office of Science, Office of Basic Energy Sciences under DE-SC0001299.

References

[1] Gertsman VY, Birringer R. Scr Metal Et Mater 1994;30:577.
[2] Kirchheim R. Acta Mater 2002;50:413.
[3] Weissmüller. Nanostruct Mater 1993;3:261.
[4] Weissmüller J. Mater Sci Eng A 1994;179–180:102.
[5] Krill CE, Ehrhardt H, Birringer R. Z Metallk 2005;96:1134.
[6] Chen Z, Liu F, Wang HF, Yang W, Yang GC, Zhou YH. Acta Mater 2009;57:1466.
[7] Liu F, Chen Z, Yang W, Yang CL, Wang HF, Yang GC. Mater Sci Eng A 2007;457:13.
[8] Michels A, Krill CE, Ehrhardt H, Birringer R, Wu DT. Acta Mater 1999;47:2143.
[9] Chen Z, Liu F, Yang X, Shen C, Fan Y. J Alloys Compd 2011;509:7109.
[10] Li J, Wang J, Yang G. Scr Mater 2009;60:945.
[11] Millett PC, Selvam RP, Bansal S, Saxena A. Acta Mater 2005;53:3671.
[12] Millett PC, Selvam RP, Saxena A. Acta Mater 2006;54:297.
[13] Millett PC, Selvam RP, Saxena A. Acta Mater 2007;55:2329.
[14] Rajgarhia R, Saxena A, Spearot D, Hartwig K, More K, Kenik E, et al. J Mater Sci 2010;45:6797.
[15] Rajgarhia R, Spearot D, Saxena A. Metall Mater Trans A 2010;41:854.
[16] Bedorf D, Mayr SG. Scr Mater 2007;57:853.
[17] Mayr SG, Bedorf D. Phys Rev B 2007;76:024111.
[18] Purohit Y, Sun L, Irving DL, Scattergood RO, Brenner DW. Mater Sci Eng A 2010;527:1769.
[19] Purohit Y, Jang S, Irving DL, Padgett CW, Scattergood RO, Brenner DW. Mater Sci Eng A 2008;493:97.
[20] Detor AJ, Schuh CA. Acta Mater 2007;55:4221.
[21] Mehta SC, Smith DA, Erb U. Mater Sci Eng A 1995;204:227.
[22] Hentschel T, Isheim D, Kirchheim R, Muller F, Kreye H. Acta Mater 2000;48:933.
[23] Choi P, Al-Kassab T, Gartner F, Kreye H, Kirchheim R. Mater Sci Eng A 2003;353:74.
[24] da Silva M, Klement U. Z Metallk 2005;96:1009.
[25] Talin AA, Marquis EA, Goods SH, Kelly JJ, Miller MK. Acta Mater 2006;54:1935.
[26] Darling KA, VanLeeuwen BK, Koch CC, Scattergood RO. Mater Sci Eng A 2010;527:3572.
[27] Thuvander M, Abraham M, Cerezo A, Smith GDW. Mater Sci Technol 2001;17:961.
[28] Darling KA, Chan RN, Wong PZ, Semones JE, Scattergood RO, Koch CC. Scr Mater 2008;59:530.
[29] Chen X, Mao J. J Mater Eng Perform 2011;20:481.
[30] da Silva M, Wille C, Klement U, Choi P, Al-Kassab T. Mater Sci Eng A 2007;445–446:31.
[31] Detor AJ, Schuh CA. J Mater Res 2007;22:3233.
[32] Detor AJ, Schuh CA. Acta Mater 2007;55:371.
[33] Färber B, Cadel E, Menand A, Schmitz G, Kirchheim R. Acta Mater 2000;48:789.
[34] Choi P, da Silva M, Klement U, Al-Kassab T, Kirchheim R. Acta Mater 2005;53:4473.
[35] Kirchheim R. Acta Mater 2007;55:5129.
[36] Meng QP, Rong YH, Hsu TY. Mater Sci Eng A 2007;471:22.
[37] Darling KA, VanLeeuwen BK, Semones JE, Koch CC, Scattergood RO, Kecskes LJ, et al. Mater Sci Eng A 2011;528:4365.
[38] Trelewicz JR, Schuh CA. Phys Rev B: Condens Matter Mater Phys 2009;79:094112.
[39] Chookajorn T, Murdoch HA, Schuh CA. Science 2012;337:951.
[40] Ishida K. J Alloys Compd 1996;235:244.
[41] Fultz B, Frase HN. Hyperfine Interact 2000;130:81.
[42] Li JH, Dai Y, Cui YY, Liu BX. Mater Sci Eng R 2011;72:1.